

UV–NIR restframe luminosity functions of the galaxy cluster EIS 0048 at $z \sim 0.64$ [★]

M. Massarotti, G. Busarello, F. La Barbera, and P. Merluzzi

I.N.A.F., Istituto Nazionale di Astrofisica Osservatorio Astronomico di Capodimonte, via Moiariello 16, 80131 Napoli, Italy

Received 23 December 2002 / Accepted 24 March 2003

Abstract. We derive the galaxy luminosity functions in V -, R -, I -, and K -bands of the cluster EIS0048 at $z \sim 0.64$ from data taken at the ESO Very Large Telescope. The data span the restframe wavelength range from UV, which is sensitive to even low rates of star formation, to the NIR, which maps the bulk of the stellar mass.

By comparing our data and previous results with pure luminosity evolution models, we conclude that bright ($M \leq M^* + 1$) cluster galaxies are already assembled at $z \sim 1$ and that star formation is almost completed at $z \sim 1.5$.

Key words. galaxies: clusters: individual: EIS 0048-2942 – galaxies: evolution – galaxies: luminosity function, mass function – galaxies: photometry

1. Introduction

One of the main issues in theoretical and observational research is to understand the physical processes driving the formation and evolution of bright massive galaxies in clusters, and to constrain the relative time scales.

The evolution of the cluster galaxy sequence (the colour–magnitude relation) has been studied for large cluster samples up to redshift $z \sim 1$ (Aragon–Salamanca et al. 1993; Lubin 1996; Ellis et al. 1997; Stanford et al. 1998, hereafter SED98; Nelson et al. 2001, hereafter NGZ01). The results are consistent with a monolithic collapse scenario (see e.g. Larson 1974) in which galaxies form at high redshifts and subsequently undergo passive evolution. However, the evolution of colours only inform on the epoch when the bulk of stellar mass formed, while cluster bright galaxies ($M \leq M^* + 1$, mostly early–type) could have been also assembled recently ($z < 1$) from mergers of smaller units, at least as long as the merging processes do not induce strong star formation.

A different approach consists in the study of the evolution of the cluster luminosity function (CLF). In particular, the near–infrared (NIR) CLF can be used to assess the assembly history of galaxies, because the NIR light mainly informs on galaxy mass. From the analysis of the values of M^* in the K -band as a function of redshift for a sample of 38 clusters in the range $0.1 < z < 1$, De Propris et al. (1999, hereafter DPSE99) found a trend consistent with passive luminosity evolution (PLE) (see also Nakata et al. 2001, hereafter

NKY01). DPSE99 conclude that the mass function of bright cluster galaxies is invariant at $z < 1$, and that the assembly of those galaxies is largely complete by $z \sim 1$. Spectroscopic data also show that massive galaxies already exist at least up to $z = 0.83$ (van Dokkum et al. 1998).

In this work we derive the CLFs for EIS 0048 at $z \sim 0.64$ in the V -, R -, I -, and K -bands (UV to NIR restframe). The cluster membership has been assessed with the photometric redshift technique up to $M - M^* \sim 1.5$ – 2.5 (according to the different depth of each band). Since no other selection has been applied, the samples are not biased toward a particular galaxy population.

The paper is organized as follows. In Sect. 2 we introduce the photometric data, discuss the background subtraction, the selection of cluster members, the completeness of the samples, and obtain the CLFs. In Sect. 3 we discuss the results in terms of galaxy formation and evolution. In Sect. 4 we give a summary of the paper. In this work we assume $H_0 = 70 \text{ km s}^{-1} \text{ Mpc}^{-1}$, $\Omega_M = 0.3$ and $\Omega_\Lambda = 0.7$.

2. Derivation of the luminosity functions

The photometric observations of the cluster of galaxies EIS0048 were carried out at the ESO Very Large Telescope (VLT) during two observing runs on August 2001. All the nights were photometric with excellent seeing conditions.

The data include $VRIK$ imaging taken with the FORS2 and ISAAC instruments, respectively. The VRI images consist of a single pointing of $6.8 \times 6.8 \text{ arcmin}^2$ for each band, while for the K -band a mosaic of four pointings covers a total area of $4.9 \times 4.9 \text{ arcmin}^2$. Further details on the observations and on the data

Send offprint requests to: M. Massarotti,
e-mail: michele@na.astro.it

[★] Based on observations collected at the European Southern Observatory.

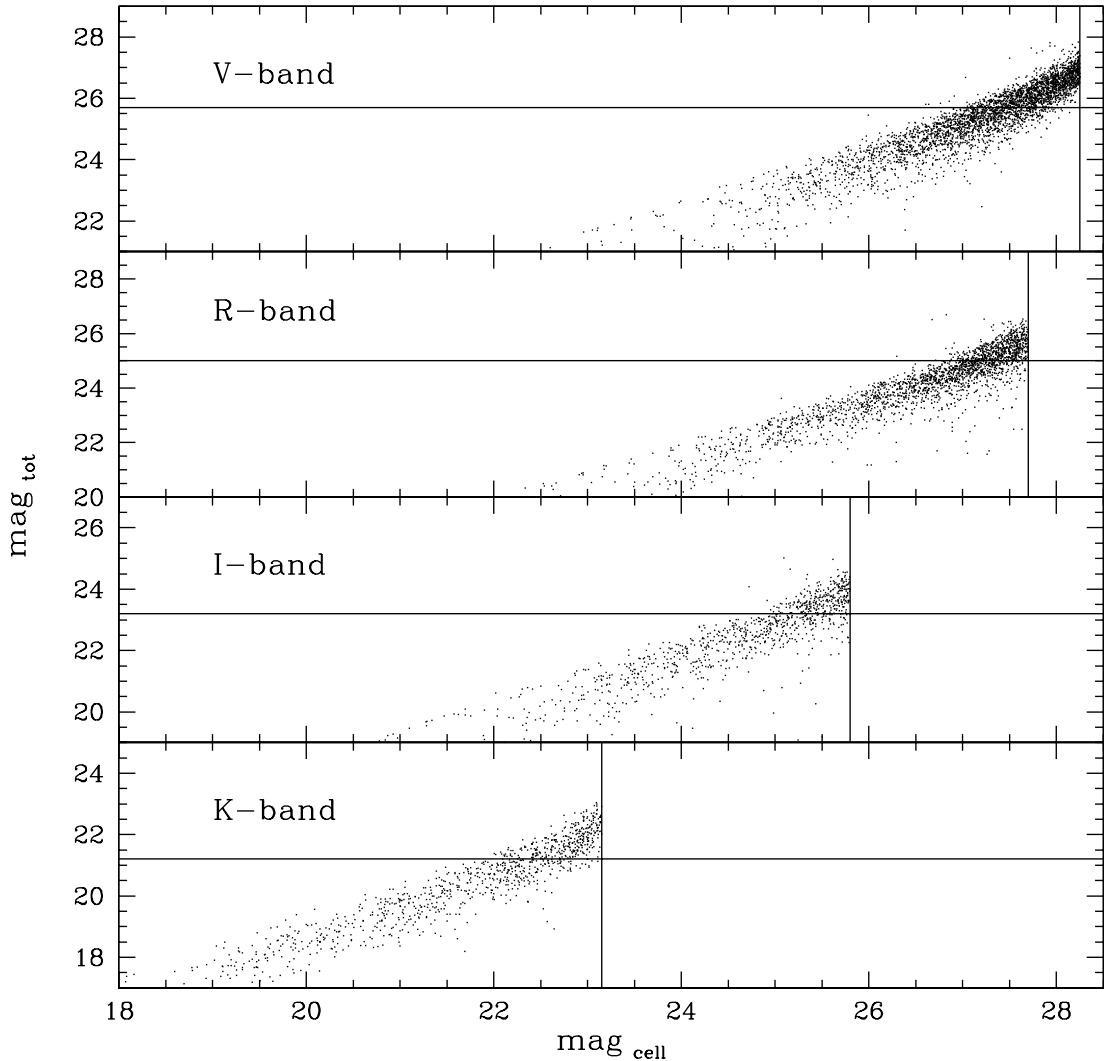


Fig. 1. Completeness limits of the photometric catalogues. Total magnitudes (mag_{tot}) are plotted against the magnitudes in the detection aperture (mag_{cell}). The vertical and horizontal lines correspond to the detection threshold and to the completeness magnitudes respectively.

reduction can be found in La Barbera et al. (2003, hereafter LBMI03).

2.1. Magnitudes and completeness

Total magnitudes were computed by means of the software SExtractor (Bertin & Arnouts 1996). For each object we obtained Kron magnitudes (m_K) within an aperture of diameter $\alpha \cdot r_K$, where r_K is the Kron radius (Kron 1980). We chose $\alpha = 2.2$, for which m_K is expected to enclose 92% of the total flux, and we computed the total magnitudes by adding 0.08 mag to m_K (see LBMI03 for details).

The formal completeness of the catalogues was estimated following the method of Garilli et al. (1999, see also Busarello et al. 2002). This method consists in the determination of the magnitude at which the objects start to be lost since they are below the brightness threshold in the detection cell¹. To estimate the completeness limit, magnitudes in the detection cell were

¹ In the present case, the detection cell is an aperture with diameter of 5 pixels.

Table 1. The completeness magnitudes. m^c is the completeness magnitude as estimated on the photometric catalogues according to Garilli et al. (1999). m_{zp}^c defines the central position of the faintest magnitude bin with completeness higher than 50% in the sample with photometric redshifts (see Sect. 2.2). The bin width is 0.5 mag.

Band	m^c mag	m_{zp}^c mag
V	25.7	24.25
R	25.0	23.25
I	23.2	22.75
K	21.2	19.75

compared to the total magnitudes. The comparisons are shown in Fig. 1, where the vertical lines correspond to the detection threshold and the horizontal lines mark the completeness limits (taking into account the scatter of the relation). The completeness magnitudes are reported in Table 1.

2.2. Background subtraction

The LFs of cluster galaxies at low and intermediate redshifts are usually obtained by statistical subtraction of the background and foreground contribution (as derived from a control field) to the galaxy counts in the cluster field. In this way all the photometric data up to the magnitude limit can be used. On the other hand, some problems become severe as the cluster redshift increases: a) cluster galaxies become fainter; b) the number of galaxies in the control field becomes higher; c) clusters are younger and therefore the number of cluster galaxies is smaller. The consequences are that the contrast of cluster galaxies over the field decreases as a function of redshift, and that the Poissonian fluctuations of the field as well as field-to-field variations become higher than the signal to be detected (see also NKY01).

To analyse this problem, we compare a known CLF translated to different redshifts, with the uncertainties on field galaxy counts. We use the LF of the rich cluster AC 118 at $z = 0.31$, $N_{\text{CLU}}(m)$, in the K -band from Andreon (2001), and the galaxy counts $N_{\text{HDFS}}(m)$ and $N_{\text{CDF}}(m)$ from two different control fields: the Hubble Deep Field South (HDFS) and the Chandra Deep Field (CDF) respectively, as obtained by Saracco et al. (2001).

We define the *cluster signal-to-noise ratio* $CSNR$ as:

$$CSNR(m) = \frac{N_{\text{CLU}}(m)}{\sqrt{(N_{\text{HDFS}}(m) - N_{\text{CDF}}(m))^2 + N_{\text{CLU}}(m)}}, \quad (1)$$

where $N_{\text{CLU}}(m)$ is the signal we aim to measure and $\sqrt{(N_{\text{HDFS}}(m) - N_{\text{CDF}}(m))^2 + N_{\text{CLU}}(m)}$ is an estimate of the uncertainties on the field galaxy counts plus the Poissonian errors on the CLF.

We computed the $CSNR$ for AC 118 at $z = 0.31$ (filled circles and continuous line in Fig. 2) and then shifted it to $z = 0.64$ (open squares and dotted line) according to the PLE model described in Sect. 3. As can be seen in Fig. 2, for $z = 0.31$ $CSNR(m) > 2$ at all magnitudes and $CSNR(m) > 3$ at $m > M^* + 0.5$ ($M^* = 15.3$, see Andreon 2001). At $z = 0.64$, $CSNR(m) \leq 2$ at all magnitudes, implying that the signal to be detected would be almost equal to the noise.

An additional problem arises from two facts: a) AC 118 is a cluster richer than EIS 0048; b) by shifting the LF of AC 118 at a higher redshift, we overestimated the actual number of detected galaxies. As consequence, our estimate of $CSNR(m)$ at $z = 0.64$ must be considered as an upper limit, and adopting the procedure of statistically subtracting the background and foreground contribution from a control field would prevent an accurate estimate of the CLFs. It should also be noted that we do not have access to a control field in the immediate proximity of EIS 0048 in order to minimize uncertainties from field-to-field variations (as in NGZ01), and that we cannot derive a cumulative LF by combining the signals from different clusters at similar redshifts (as in DPSE99).

Therefore, in order to increase the contrast of cluster galaxies over field galaxies, the following approach was adopted. We first selected the cluster members through the photometric redshift technique, as detailed in LBMI03. In this way it is possible to isolate galaxies in a narrow interval $\Delta z \pm 0.1$ around the

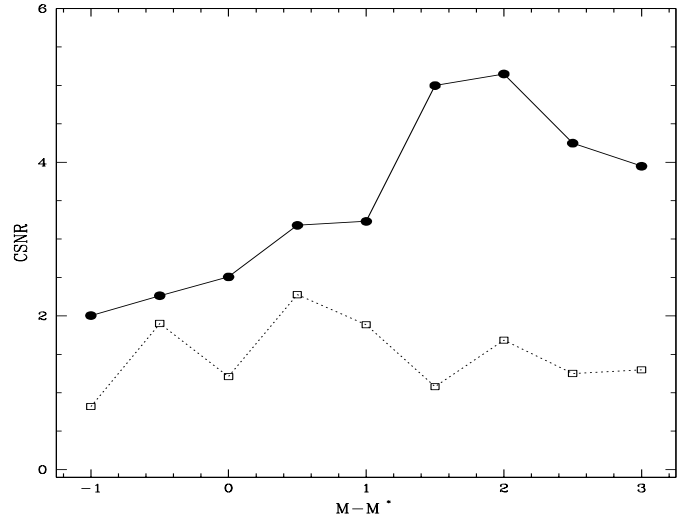


Fig. 2. The cluster signal-to-noise ratio (see text and Eq. (1)) in a rich cluster at $z = 0.31$ (filled dots and continuous line) and at $z = 0.64$ (open squares and dotted line).

cluster redshift, thus greatly decreasing the noise produced by field galaxies, while leaving the signal untouched.

To achieve a reasonable accuracy in the redshift estimate, we considered only galaxies with signal-to-noise ratio $S/N > 5$ in at least three bands. For each band, we computed the completeness function of the sample as the ratio of the number of galaxies with $S/N > 5$ in at least three bands to the total number of galaxies in the catalog, as a function of the magnitude (see Fig. 3). The CLFs have been computed in each band by considering all the galaxies with photometric redshift up to the last magnitude bin with completeness higher than 50%, as reported in Table 1. Galaxy counts have been corrected for the estimated incompleteness.

After the previous selection, field contamination is still present in the peak of the redshift distribution around $z = 0.64$. To account for the remaining contamination, we took advantage of the VIRMOS preparatory photometric survey as control sample (see LBMI03). By selecting galaxies in the redshift range $z \in [0.54, 0.74]$ (LBMI03) in the VIRMOS control field, we obtained the luminosity distribution of contaminant galaxies, and subtracted it from galaxy counts in the same redshift range in the cluster field. At $K \leq 20$ the ratio of cluster to field galaxies without any photometric redshift selection is ~ 0.5 (from Saracco et al. 2001 data in the CDF), whereas the same ratio after the photometric redshift selection is ~ 6.6 (from the VIRMOS data), thus proving the effectiveness of our procedure.

2.3. Luminosity functions

We modelled the CLFs with a weighted parametric fit of the Schechter function, fixing the faint end slope to have $\alpha = -0.9$. We chose not to fit α because the samples with photometric redshifts are only complete to $M - M^* = 1.5-2.5$ (according to the band). Moreover, $\alpha = -0.9$ is the value measured in the NIR for the Coma cluster at $K < K^* + 3$ (De Propris et al. 1998) and is also the value adopted by DPSE99 to study

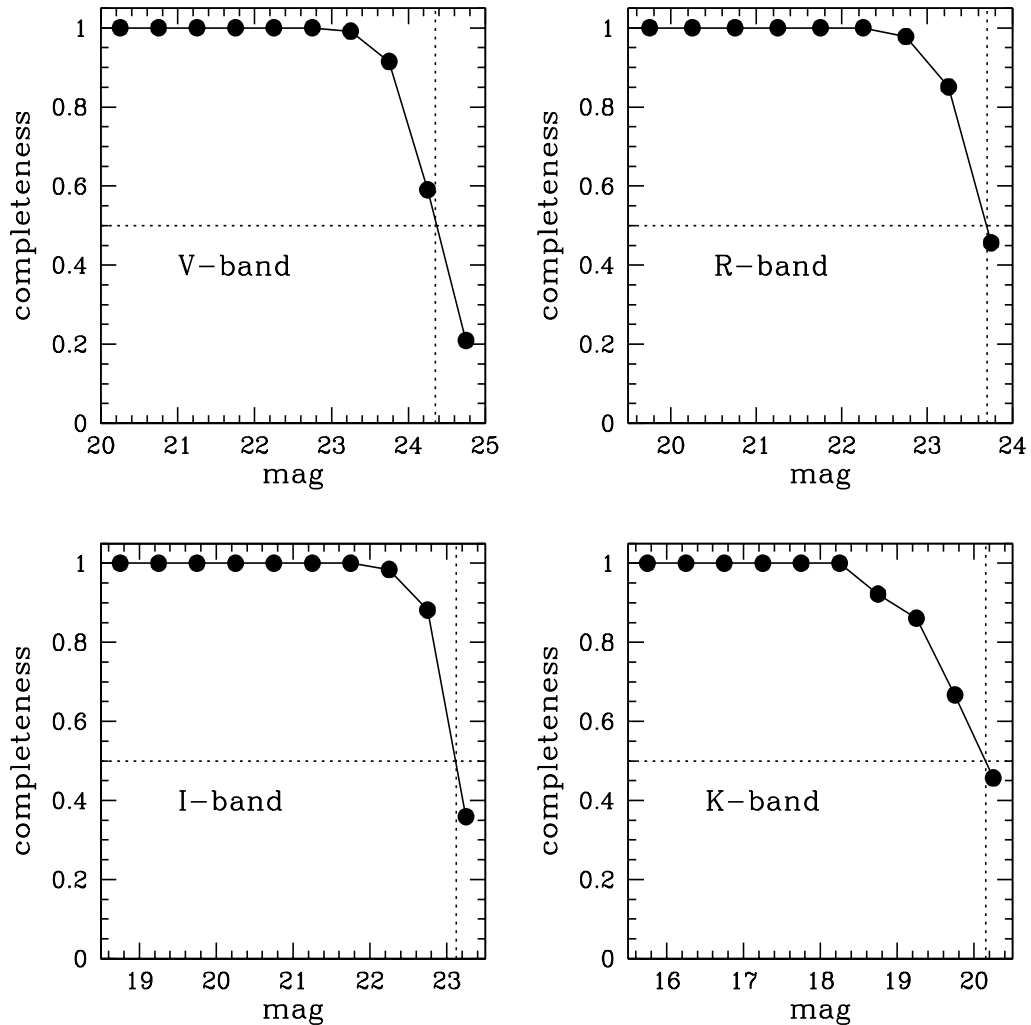


Fig. 3. The completeness as a function of the magnitude of the samples used to derive the photometric redshift distribution of the galaxies in the EIS0048 field. In each panel the vertical dotted line indicates the magnitude corresponding to 50% completeness. The CLFs are computed up to the faintest magnitude bin brighter than these limits.

the behaviour of K^* as a function of the redshift. The errors on the CLFs were computed by taking into account Poissonian fluctuations of cluster galaxies counts and of the background counts in the redshift range $z \in [0.54, 0.74]$. In Fig. 4 we show the CLFs from V - to K -band (filled circles) and the best-fitting Schechter functions (solid lines). The values of M^* computed by the fits are listed in Table 2.

In the K -band we obtain $M^* = 17.18 \pm 0.23$, in agreement within the errors with the result of DPSE99 at the same redshift ($K^* = 17.57 \pm 0.41$). By comparing the values of M^* in I - and K -band, we obtain $I^* - K^* = 3.06 \pm 0.28$ for the bright cluster galaxies at $z = 0.64$, in agreement with the findings of SED98 and NGZ01 at similar redshifts.

3. Luminosity evolution of bright ($M \leq M^* + 1$) cluster galaxies

We discuss the luminosity evolution of bright galaxies in clusters on the basis of the behaviour of the V - and K -bands characteristic magnitudes M^* with redshift. Complementary data for the K -band are taken from DPSE99, Andreon (2001), and

Table 2. The values of M^* computed from the fits of the Schechter function to the CLFs of EIS0048. M^* is obtained by fixing $\alpha = -0.9$.

Band	M^*
V	22.70 ± 0.25
R	21.27 ± 0.20
I	20.24 ± 0.18
K	17.18 ± 0.23

NKY01, while for the V -band are taken from Busarello et al. (2002). The different data sets are represented in Fig. 5 with different symbols. The points at $z = 0.31$ in the K - and V -band are obtained from the luminosity functions of Andreon (2001) and Busarello et al. (2002), assuming $\alpha = -0.9$ up to $M \sim M^* + 2$. In this way all the numerical estimates of M^* have been obtained with the same value of α and can be straightly compared.

In Fig. 5 no-evolution (NE, pure k -correction) and PLE models are also shown. The galaxy models are constructed

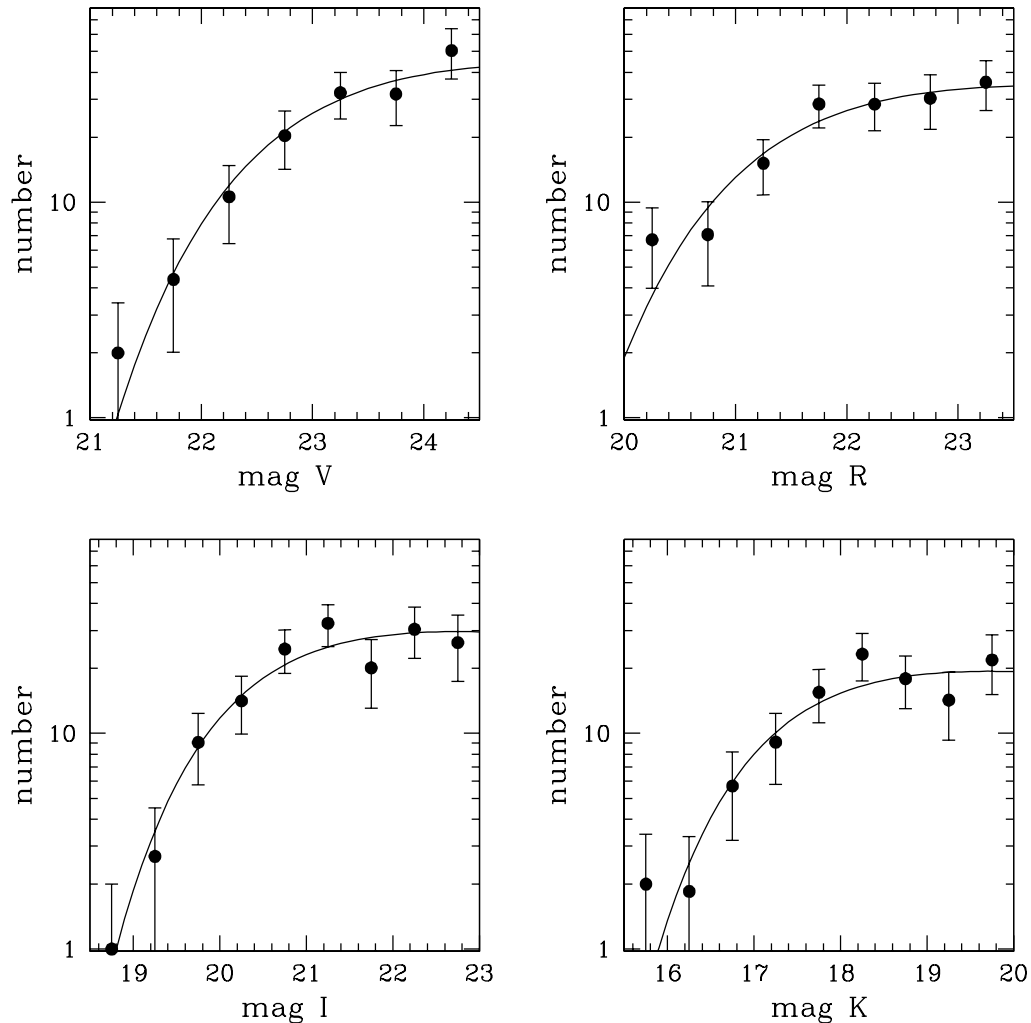


Fig. 4. The CLFs of EIS 0048 from V- to K-band (filled dots). In each panel the best-fit Schechter function is also shown (solid line).

using Bruzual & Charlot (1993) templates with a Scalo initial mass function, solar metallicity, and an exponential star formation law $e^{-t/\tau}$. We assumed the time scale $\tau = 1$ Gyr, which is suitable to reproduce the colour evolution of early type galaxies (see Bruzual & Charlot 1993; Merluzzi et al 2003). The NE predictions use model spectra with formation redshift $z_f = 5$ (the redshift of the onset of SF). The predictions from PLE are given for different z_f . All the models are normalized to $K^* = 10.90$ and $V^* = 14.17$ at the redshift of Coma (Bower et al. 1992; De Propris et al. 1998).

As widely discussed in literature (e.g. DPSE99; NKY01), the behaviour of K^* is inconsistent with a NE model. Our data points at $z = 0.64$ confirm this result (at $\sim 2.5\sigma$), and extend it in the V-band (at $\sim 4\sigma$). The evolution in the K-band can be described by PLE models at least up to $z \sim 1$ (the point at $z = 1.2$ in Fig. 5 should be taken with caution since NKY01 were not able to estimate the field contamination). Since the K-band samples the bulk of stellar mass, this result suggests that the assembly of bright galaxies in clusters is complete at $z \sim 1$ (DPSE99).

The K-band data alone cannot discriminate among models with different formation redshifts. At $z = 0.64$ the V-band

samples the UV restframe and is therefore sensitive to even low levels of star formation activity. As can be seen in the upper right panel in Fig. 5, the evolution of V^* is in agreement with PLE models with $z_f \geq 3$. This result depends on the time scale of star-formation history, but we can use our point at $z = 0.64$ in the V-band to constrain the time when galaxies ceased to form stars. This is possible because the magnitude evolution subsequent to this time is almost independent from the preceding star-formation history.

In the lower panels of Fig. 5 we plot the PLE models corresponding to the different epochs at which galaxies formed 99% of their present stars. As it is apparent from the figure, the V-band data constrain the star formation in cluster bright galaxies to end at $z \geq 1.5$.

4. Summary and conclusions

We derived the galaxy LF in V-, R-, I-, and K-bands of the cluster EIS 0048 at $z \sim 0.64$ from new photometric observations carried out at ESO VLT with FORS2 and ISAAC. Cluster members have been selected with the photometric redshift technique in order to enhance the contrast among

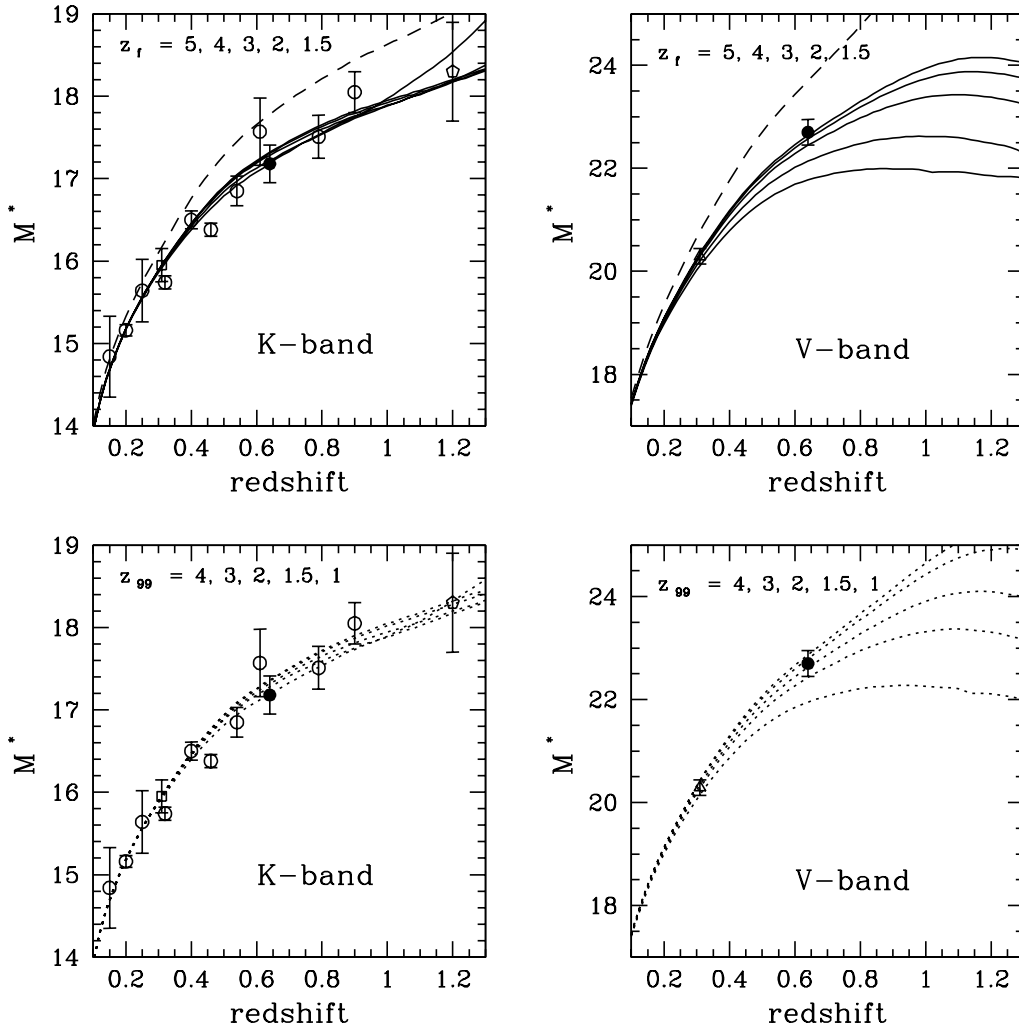


Fig. 5. Evolution of the Schechter parameter M^* in K - and V -bands as a function of redshift. In the K -band the data come from DPSE99 (empty circles), Andreon (2001, empty square), NKY01 (empty pentagon), and from this work (filled circle). In the V -band the data come from Busarello et al. (2002, empty triangle) and from this work (filled circle). In the upper panels, the dashed lines represent the NE model. The PLE models (solid lines) at different formation redshift z_f are shown in decreasing order of z_f from top to bottom. In the lower panels the PLE models (dotted lines) are shown as a function of the redshift z_{99} at which galaxies formed the 99% of their stars (decreasing from top to bottom).

cluster- and background-foreground galaxies. The remaining field contamination has been estimated as detailed in LBMI03.

The CLFs have been obtained up to $M - M^* \sim 1.5-2.5$ (according to the waveband). We modelled the CLFs with a weighted parametric fit of the Schechter function, fixing the faint end slope to be $\alpha = -0.9$. The values of M^* obtained in I - and K -bands are in agreement with the analysis of DPSE99 and NGZ01 at similar redshifts. We collected results from literature and introduced PLE models with different formation redshifts in order to discuss the evolution of M^* in the V - and K -bands. The key factors driving the evolution of bright galaxies in the scenario of hierarchical structure formation are the epoch when the bulk of stellar populations is formed, the cosmological time when mergers are effective to assemble the galaxies, the amount of star formation induced by mergers, and the age of the youngest stars. Since the evolution of K^* is consistent with a PLE scenario at least up to $z \sim 1$, we can conclude that mergers must have already assembled bright ($M \leq M^* + 1$)

cluster galaxies at this redshift (see also DPSE99 for a thorough discussion). At $z = 0.64$ the V -band samples the UV rest-frame wavelength region and is sensitive to even low levels of SF. We find that the SF in bright cluster galaxies has to be almost completed at $z \sim 1.5$, whereas the formation redshift is $z_f \geq 3$ assuming $\tau \sim 1$ Gyr as the time scale for SF. These results lead to conclude that the structure and the stars of bright cluster galaxies must have been formed between $z = 4 \pm 1$ and $z = 1.2 \pm 0.2$.

Acknowledgements. We are grateful to C. Lidman who helped us for the K -band photometric calibration, and thank the ESO staff who effectively attended us during the observation runs at Paranal. We warmly thank the VIRMOS Consortium who allowed us to use a subset of VIRMOS photometric data base to estimate the field contribution in LBMI03. We thank the unknown referee for his/her useful comments. Michele Massarotti is partly supported by a MIUR-COFIN grant.

References

- Andreon, S. 2001, *ApJ*, 547, 623
- Aragón-Salamanca, A., Ellis, R. S., Couch, W. J., & Carter, D. 1993, *MNRAS*, 262, 764
- Bertin, E., & Arnouts, S. 1996, *A&AS*, 117, 393
- Bower, R. G., Lucey, J. R., & Ellis, R. S. 1992, *MNRAS*, 254, 601
- Bruzual, G. A., & Charlot, S. 1993, *ApJ*, 405, 538
- Busarello, G., Merluzzi, P., La Barbera, F., Massarotti, M., & Capaccioli, M. 2002, *A&A*, 389, 787
- De Propris, R., Eisenhardt, P. R., Stanford, S. A., & Dickinson, M. 1998, *ApJ*, 503, L45
- De Propris, R., Stanford, S. A., Eisenhardt, P. R., Dickinson, M., & Elston, R. 1999, *AJ*, 118, 719
- Ellis, R. S., Smail, I., Dressler, A., et al. 1997, *ApJ*, 483, 582
- Garilli, B., Maccagni, D., & Andreon, S. 1999, *A&A*, 342, 408
- Kron, A. U. 1992, *AJ*, 104, 340
- La Barbera, F., Merluzzi, P., Iovino, A., Massarotti, M., & Busarello, G. 2003, *A&A*, 399, 899
- Larson, R. B. 1974, *MNRAS*, 166, 585
- Lubin, L. 1996, *AJ*, 112, 23
- Merluzzi, P., La Barbera, F., Massarotti, M., Busarello, G., & Capaccioli, M. 2003, *ApJ*, in press [[astro-ph/0206403](https://arxiv.org/abs/astro-ph/0206403)]
- Nakata, F., Kajisawa, M., Yamada, T., et al. 2001, *PASJ*, 53, 1139
- Nelson, A. E., Gonzalez, A. H., Zaritsky, D., & Dalcanton, J. J. 2001, *ApJ*, 563, 629
- Saracco, P., Giallongo, E., Cristiani, S., et al. 2001, *A&A*, 375, 1
- Stanford, S. A., Eisenhardt, P. R. M., & Dickinson, M. 1998, *ApJ*, 492, 461
- van Dokkum, P. G., Franx, M., Kelson, D. D., & Illingworth, G. D. 1998, *ApJ*, 504, L17